51-7; [Co(salen)Na(CO_2)], 82570-84-1; [Co(salen)]K, 82536-92-3; [(Py)Co(salen)K(CO_2)], 82536-93-4; [Co(salen)Cs(CO_2)], 82570-85-2; [Co(Et-salen)Li(CO_2)], 82536-94-5; [Co(Et-salen)Na(CO_2)], 82536-95-6; [Co(Pr-salen)K(CO_2)(THF)], 82536-97-8; [Co(salen)Na]$_2$-(DCHC), 82536-99-0.

Supplementary Material Available: A listing for structure factor amplitudes for complexes [Co(*n*-Pr-salen)K(CO_2)(THF)] (form A), [Co(*n*-Pr-salen)K(CO_2)(THF)] (form B), and complex V; Interatomic distances for (*n*-Pr-salen) ligand are listed in Table VIII (form A) and Table IX (form B); calculated fractional atomic coordinates for hydrogen atoms of form B (Table X) and of complex V (Table XI); bond distances and angles for the Co(salen) group in complex V (Table XII) (14 pages). Ordering information is given on any current masthead page.

Synthetic, Structural, and Physical Studies of Bis(triethylammonium) Tris(catecholato)vanadate(IV), Potassium Bis(catecholato)oxovanadate(IV), and Potassium Tris(catecholato)vanadate(III)

Stephen R. Cooper,*[1] Yun Bai Koh,[2] and Kenneth N. Raymond*[2,3]

Contribution from the Departments of Chemistry, Harvard University, Cambridge, Massachusetts 02138, and the University of California, Berkeley, California 94720. *Received August 6, 1981*

Abstract: The syntheses, properties, and crystal structures of the complexes $[Et_3NH]_2[V(cat)_3]\cdot CH_3CN$, $K_3[V(cat)_3]\cdot 1.5H_2O$, and $K_2[VO(cat)_2]\cdot EtOH\cdot H_2O$ are described. The complex $[Et_3NH]_2[V(cat)_3]\cdot CH_3CN$ [$P2_12_12_1$, with a = 10.473 (1) Å, b = 10.794 (1) Å, and c = 29.986 (3) Å; Z = 4; ρ_{calcd} = 1.216; ρ_{obsd} = 1.21 g cm^{-3}; R_w = 7.2%] consists of a novel vanadium(IV) octahedral complex [V–O bond length 1.930 (3) Å; O–V–O bond angle 88.8°] in which catechol has displaced the vanadyl oxygen. In contrast, $K_2[VO(cat)_2]\cdot EtOH\cdot H_2O$ [$P2_1/c$ with a = 14.380 (1) Å, b = 12.307 (2) Å, and c = 11.187 (1) Å, β = 111.80°; Z = 4; ρ_{calcd} = 1.537; R_w = 7.8%] is a typical square-pyramidal vanadyl complex: V=O bond length of 1.616 (4) Å, the vanadium 0.58 Å out of the basal plane, and average V–O(catechol) bond lengths of 1.956 Å. The complex $K_3[V(cat)_3]\cdot 1.5H_2O$ [$C2/c$, with a = 20.727 (4) Å, b = 15.884 (2) Å, c = 12.312 (2) Å, and β = 91.46°; Z = 8; ρ_{calcd} = 1.703; R_w = 4.6%] closely approximates octahedral symmetry about the metal and is isostructural with the Cr and Fe analogues. In addition to the synthesis and structures of these complexes, we report the results of optical, infrared, and electron paramagnetic resonance spectroscopy, as well as electrochemical and magnetic studies for the complexes VOL, VOL_2, and VL_3 (where L = catechol, 4,5-dihydroxybenzene-1,3-disulfonate and 3,5-di-*tert*-butylcatechol). The unprecedented feature of these results is observation of a tris octahedral structure for a vanadium(IV) complex in water. This remarkable displacement of the vanadyl oxygen is attributable to the exceptional chelating ability of catechol and its great affinity for highly charged metal ions—similar to that of hydroxide. The extensive, and often contradictory, literature of this field is reconciled and the claims for reversible O_2 binding by a V(IV) catecholate species are shown to be spurious.

As part of our studies of transition-metal complexes with siderophores,[4] in particular those of the catechol (*o*-dihydroxybenzene) type, we have been led to include studies of the parent ligand, catechol itself. In the present report the interaction of catechol with vanadium is described, an interaction which, despite having seen numerous studies, is still characterized by confusion in the literature. The failure to isolate and characterize complexes structurally has largely been responsible for the puzzlement about whether vanadium(IV) forms a tris complex with catechol or a vanadyl bis(catecholate) and the question of whether the V(V) complex is capable of existence. Despite this confusion, the deep blue color produced by interaction of V(IV) or V(V) with catechol has been of analytical value,[5] even though the nature of the blue species was unclear.

Early studies by Rosenheim and Mong[6] led these workers to suggest for their deep blue product a vanadyl bis(catecholate) structure with a catechol of crystallization, apparently in the belief that the very stable vanadyl group could not be displaced.

This belief subsequently appeared to be supported by numerous[7-11] potentiometric studies, in which an end point was found at 4 mol of alkali/mol of vanadium (independent of the catechol/vanadium ratio); this was taken to indicate that the terminal member of the coordination series was the vanadyl bis(catecholate).

However, in contradiction to this conclusion, Henry, Mitchell, and Prue[12] in the definitive work to date found that thallous salts precipitated a complex, which analysis indicated is the tris complex $Tl_2[V(cat)_3]$ (with 1.7 μ_B magnetic moment) but which unfortunately is completely insoluble in solvents with which it does not react.

Despite the isolation of complexes with 3:1 ligand:metal stoichiometry by Rosenheim et al. and by Henry et al., another potentiometric study by the latter authors[13] also failed to provide

(1) Department of Chemistry, Harvard University, Cambridge, MA 02138.
(2) Department of Chemistry, University of California, Berkeley, CA 94720.
(3) Address correspondence to this author at U. C. Berkeley.
(4) Raymond, K. N.; Carrano, C. J. *Acc. Chem. Res.* **1979**, *12*, 183-190.
(5) Nardillo, A. M.; Catoggio, J. A. *Anal. Chim. Acta* **1975**, *74*, 85-99 and references therein.
(6) Rosenheim, A.; Mong, Z. *Z. Anorg. Allg. Chem.* **1925**, *148*, 25-34.
(7) Trujillo, R.; Brito, F.; Cabrera, J. *Chem. Abstr.* **1959**, *51*:4800.
(8) Beltran-Martinez, T.; Mateo, L. L. *Chem. Abstr.* **1966**, *64*:15065.
(9) Lal, K.; Agarwal, R. P. *Bull. Chem. Soc. Jpn.* **1967**, *40*, 1148-1152.
(10) Husein, G. M.; Bhattacharya, P. K. *J. Indian Chem. Soc.* **1969**, *46*, 875-878.
(11) Zelinka, J.; Bartusek, M. *Collect. Czech. Chem. Commun.* **1971**, *36*, 2615-2624.
(12) Henry, R. P.; Mitchell, P. C. H.; Prue, J. E. *J. Chem. Soc. A* **1971**, 3392-3395.
(13) Henry, R. P.; Mitchell, P. C. H.; Prue, J. E. *J. Chem. Soc., Dalton Trans.* **1973**, 1156-1159.

0002-7863/82/1504-5092$01.25/0

potentiometric evidence for vanadium(IV) tris(catecholate). Zelinka and Bartusek[11] and Henry, Mitchell, and Prue[13] noted that none of the reported potentiometric data agreed with a spectrophotometric report[14] that at pH 3–4 an initial 2:1 complex converts to a tris complex over a period of several minutes.

Greater agreement was achieved on the question of oxidation state of the vanadium–catecholate complexes—it was widely agreed that V(V) catechol complexes were unstable with respect to internal redox reaction. Shnaiderman et al.[15,16] and Zelinka et al.[17] reported that reaction of vanadate with catechol in solutions with $3 < pH < 10$ gave a V(IV) species with $\lambda_{max} = 580$ nm and the eight-line electron paramagnetic resonance spectrum characteristic of ^{51}V ($I = {}^7/_2$, 100%). From the EPR spectra, they concluded that catechol reduced vanadate quantitatively under these conditions, as it does in solutions of low pH,[18,19] and that therefore V(V) catechol complexes could not exist. However, it is now known that even such powerful oxidants as Ce(IV) can form stable complexes with catechol, apparently without oxidation of the ligand.[20] In addition, observation of a V(IV) EPR spectrum does not necessarily imply complete reduction of V(V) by catechol—either partial reduction or even adventitious V(IV) would yield the same result—and in neither study were the requisite magnetic measurements performed to establish the extent of reduction. Shnaiderman et al. also reported that a neutral yellow "complex" ($\lambda_{max} = 380$ nm), which was extracted by ethylene chloride, was also produced by reaction of V(V) with catechol; however, it is now clear that the yellow "complex" is simply *o*-benzoquinone,[5] which is formed by air in a process that may be catalyzed by the metal.

We report here the successful synthesis, isolation, and X-ray structural determination of the elusive deep blue complex of vanadium(IV) with catechol, the results of which establish that this latter complex is a tris(catecholato) *octahedral* species. We further wish to report the synthesis and structural characterization of the previously postulated vanadyl bis(catecholate) and that of the vanadium(III) tris(catecholate). In addition, we have characterized by optical and electron paramagnetic resonance, as well as by magnetic and electrochemical means, the mono, bis, and tris V(IV) complexes of the related ligands Tiron (sodium 4,5-dihydroxy-1,3-benzenedisulfonate) and 3,5-di-*tert*-butylcatechol, as well as the mono complex of catechol, and the diamagnetic V(V) tris complexes with catechol and 3,5-di-*tert*-butylcatechol. Having done so, we can now account satisfactorily for all previous observations reported in the literature.[52]

Recently Sawyer and co-workers[21] published a report that a vanadium(IV)–catechol complex of 1:2 stoichiometry reversibly binds O_2, NO, and CO in methanolic solution. The oxygen-binding species was claimed to be a *tetrahedral* vanadium(IV) complex—an unprecedented coordination geometry for vanadium(IV) in a donor solvent. Our skepticism about this report prompted us to extend the present study to examine these claims, in which they are demonstrated to be spurious.

Experimental Section

Vanadyl acetylacetonate [$VO(acac)_2$] was prepared by the literature procedure[22] and recrystallized from chloroform–acetone. Catechol was recrystallized from benzene, while benzoquinone was sublimed before use. Ammonium metavanadate was recrystallized as described by Brauer.[23] Methanol was distilled from magnesium methoxide, triethylamine from BaO, and acetonitrile from CaH_2. Other chemicals were reagent grade and were used as received.

Physical Measurements. Infrared spectra were obtained as KBr pellets on a Perkin-Elmer 283 grating spectrometer, with poly(styrene) as frequency calibrant. Optical spectra were measured in septum-sealed quartz cuvettes with Perkin-Elmer 558A or 554 or Cary 118 spectrophotometers. Electron paramagnetic resonance (EPR) spectra were recorded with a Varian E-9 spectrometer with diphenylpicrylhydrazyl radical (DPPH) as *g* marker ($g = 2.0037$); quartz flat cells were used for fluid solutions, while cylindrical quartz tubes were employed for frozen solutions. Electrochemical experiments were performed with a Princeton Applied Research (PAR) 173 potentiostat, 175 programmer, 179 coulometer, and Houston 2000 x–y recorder. All potentials are relative to the saturated calomel electrode (SCE) and are uncorrected for junction potentials. Platinum disk or hanging mercury drop electrodes were employed for cyclic voltammetric experiments, stirred mercury pool or platinum mesh electrodes for coulometric measurements. Acetonitrile solutions were 0.1 M in tetraethylammonium perchlorate (TEAP); aqueous solutions were 1 M in KCl. Magnetic measurements were performed on solutions in coaxial tubes by the NMR technique.[24]

Synthesis of Compounds. All operations were carried out under nitrogen atmosphere by standard syringe and Schlenk techniques unless otherwise specified.

$[Et_3NH]_2[V(cat)_3]\cdot CH_3CN$. Addition of 2.65 g (10 mmol) of $VO(acac)_2$ in 20 mL of MeOH to 6.6 g of catechol (60 mmol) in 10 mL of MeOH affords a blue-violet solution, to which 6 mL of Et_3N (distilled from BaO) was added. Upon addition of the amine the color became much more intense, as complex formation was driven to completion, and the deep blue-violet product precipitated. Recrystallization from hot CH_3CN afforded the pure product as the acetonitrile solvate, from which crystals suitable for X-ray diffraction measurements were obtained; yield, 5.0 g (81%). Anal. Calcd for $C_{32}H_{47}N_3O_6V$: C, 61.92; H, 7.63; N, 6.77; V, 8.21. Found: C, 62.1; H, 7.67; N, 6.72; V, 8.92.

$[Et_3NH][V(DTBC)_3]\cdot 1.5CH_3OH$. Ammonium metavanadate (0.5 g, 4.3 mmol) and 10 mL of Et_3N were added to 3,5-di-*tert*-butylcatechol (3.0 g, 13.5 mmol) in 50 mL of MeOH. After reflux for 5 h and concentration to 20 mL, the dark blue product was filtered and rinsed twice with 5-mL portions of MeOH; yield, 0.6 g (16%). Anal. Calcd for $C_{49.5}H_{82}NO_{7.5}V$: C, 69.00; H, 9.52; N, 1.63; V, 5.92. Found: C, 68.67; H, 9.12; N, 1.65; V, 5.94.

$[Et_3NH]_2[VO(DTBC)_2]\cdot 2CH_3OH$. Vanadyl acetylacetonate (1.0 g, 3.8 mmol) in 50 mL of MeOH was heated for 1 h at reflux with 3,5-di-*tert*-butylcatechol (3.0 g, 13.5 mmol) in the presence of excess Et_3N. Concentration to approximately 20 mL afforded the green crystalline product, which was filtered, rinsed with ether, and air-dried; yield, 2.1 g (72%). Anal. Calcd for $C_{42}H_{80}N_2O_7V$: C, 65.03; H, 10.32; N, 3.61; V, 6.58. Found: C, 65.13; H, 10.30; N, 3.63; V, 5.76.

$K_2[VO(cat)_2]\cdot EtOH\cdot H_2O$. Dry $VOSO_4$ (2.0 g, 12 mmol) was heated for 3 h with 30 mL of water that contained 1.0 g of KOH (15 mmol) and then cooled to 0 °C. The brown crystals were filtered and rinsed with cold water. The brown compound was added to a solution of catechol (3.0 g, 27 mmol) and KOH (4.0 g, 60 mmol) in water and refluxed overnight. The deep green solution was filtered and concentrated under vacuum to 15 mL, and 90 mL of EtOH was added. Cooling to −78 °C yielded the light blue crystalline product, which was filtered, rinsed twice with 30-mL portions of EtOH, and dried under vacuum (during which time it became light green); yield, 3.2 g (76%). Recrystallization of the green product from hot 95% EtOH afforded crystals suitable for diffraction measurements.

$K_3[V(cat)_3]\cdot 1.5H_2O$. An aqueous solution of 1.0 g (6.3 mmol) of VCl_3 was added to 2.5 g (23 mmol) of catechol in 30 mL of 15% ammonium hydroxide. The mixture was stirred for 1 h at 60 °C and cooled to 0 °C. The green product was filtered, rinsed with 15% ammonium hydroxide, and dissolved in 20 mL of aqueous 1 M KOH. The resulting solution was refluxed for 0.5 h and evaporated to a residue, which was treated with 10 mL of aqueous 1 M KOH. Slow addition of 50 mL of absolute EtOH afforded green needles of $K_3[V(cat)_3]\cdot 1.5H_2O$; yield, 2.3 g (70%).

X-ray Diffraction Data Collection

The crystallographic data are summarized in Table I. Preliminary precession photography uniquely determined the space groups of $[Et_3NH]_2[V(cat)_3]\cdot CH_3CN$ and $K_2[VO(cat)_2]\cdot EtOH\cdot H_2O$, and gave as choices *Cc* or *C2/c* for $K_3[V(cat)_3]\cdot 1.5H_2O$. Successful refinement verified *C2/c* as correct. Diffraction data on the crystals mounted in quartz capillaries were collected with an Enraf-Nonius CAD-4 diffractometer by the θ–2θ scan technique. The cell dimensions and orientation

(14) Bhattacharya, P. K.; Banerji, S. N. *Z. Anorg. Allg. Chem.* **1962**, *315*, 118–120.
(15) Shnaiderman, S. Ya.; Demidovskaya, A. N.; Zaletov, V. G. *Russ. J. Inorg. Chem. (Engl. Transl.)* **1972**, *17*, 348–350.
(16) Shnaiderman, S. Ya.; Prokof'eva, G. N.; Demidovskaya, A. N.; Klimenko, E. P. *Russ. J. Inorg. Chem. (Engl. Transl.)* **1972**, *42*, 22–26.
(17) Zelinka, J.; Bartusek, M.; Okac, A. *Collect. Czech. Chem. Commun.* **1974**, *39*, 83–91.
(18) Kustin, K.; Liu, S.-T.; Nicolini, C.; Toppen, D. L. *J. Am. Chem. Soc.* **1974**, *96*, 7410–7415.
(19) Kustin, K.; Nicolini, C.; Toppen, D. L. *J. Am. Chem. Soc.* **1974**, *96*, 7416–7420.
(20) Sofen, S. R.; Cooper, S. R.; Raymond, K. N. *Inorg. Chem.* **1979**, *18*, 1611–1616.
(21) Wilshire, J. P.; Sawyer, D. T. *J. Am. Chem. Soc.* **1978**, *100*, 3972–3973.
(22) Rowe, R. A.; Jones, M. M. *Inorg. Synth. 5*, 113–116.
(23) Brauer, G. "Handbook of Preparative Inorganic Chemistry"; p 1272.
(24) Evans, D. F. *J. Chem. Soc.* **1959**, 2003.

Table I. Crystallographic Data

formula	$(Et_3NH)_2V(cat)_3 \cdot CH_3CN$	$K_3V(cat)_3 \cdot 1.5H_2O$	$K_2VO(cat)_2 \cdot EtOH \cdot H_2O$
formula wt	620.68	519.55	424.41
space group	$P2_12_12_1$	$C2/c$	$P2_1/c$
a, Å	10.473 (1)	20.727 (4)	14.380 (1)
b, Å	10.794 (1)	15.884 (2)	12.307 (2)
c, Å	29.986 (3)	12.312 (2)	11.187 (1)
β, deg	90	91.46 (2)	111.80 (1)
vol, Å^3	3389.6	4052.0	1838.2
d_{calcd}, g/cm^3	1.216	1.703	1.537
d_{obsd}, g/cm^3	1.21		
z	4	8	4
λ	Cu Kα (1.5418 Å)	Mo Kα (0.71073 Å)	Mo Kα (0.71073 Å)
μ, cm^{-1}	27.9	11.6	11.6
cryst size, mm	0.3 × 0.27 × 0.14	0.15 × 0.26 × 0.30	0.30 × 0.27 × 0.14
indep refl	4029	4639	4214
refl coll	$+h,+k,+l$	$+h,+k,\pm l$	$+h,+k,\pm l$
unique data with $F^2 > 3\sigma(F^2)$			
2θ range, deg	2.0–120.0	3.0–55.0	3.0–55.0
final R, %	5.8	3.5	5.0
final R_w, %	7.2	4.6	7.8
GOF[a]	2.37	2.50	3.33
no. of var	352	267	202

[a] The goodness of fit is defined as $[w(|F_o| - |F_c|)^2/(n_o - n_v)]^{1/2}$, where n_o and n_v denote the number of data and variables, respectively.

matrices were determined on the diffractometer as previously described.[25] Accurate cell dimensions were derived from least-squares refinement of the setting angles of at least 20 high angle reflections. Three high-angle reflections were checked every 300 reflections as orientation standards; three strong reflections, checked every 200 reflections (or 2 h), were chosen as intensity standards and the data corrected for the slight decomposition (≈2%) observed for $K_2[VO(cat)_2] \cdot EtOH \cdot H_2O$ and $K_3[V(cat)_3] \cdot 1.5H_2O$. Both the $[Et_3NH]_2[V(cat)_3] \cdot CH_3CN$ and $K_3[V(cat)_3] \cdot 1.5H_2O$ data were corrected for absorption. After deletion of systematically absent reflections and averaging of equivalent reflections, the data for $[Et_3NH]_2[V(cat)_3] \cdot CH_3CN$, $K_2[VO(cat)_2] \cdot EtOH \cdot H_2O$, and $K_3[V(cat)_3] \cdot 1.5H_2O$ yielded 3644, 4214, and 4639 independent reflections for which $I > 3\sigma$.

Structure Solution and Refinement

Structure solution and refinement was performed either by means of Patterson maps or by direct methods, followed by alternate application of full-matrix least-squares refinement and difference Fourier maps. The programs used have been described previously.[26]

$K_2[VO(cat)_2] \cdot EtOH \cdot H_2O$. This structure was solved by direct methods; the locations of the vanadium, potassium, and oxygen atoms were determined from the E map with the highest figure of merit. The coordinates of the remaining atoms were deduced by means of alternate cycles of difference Fourier synthesis and least-squares refinement. Catechol ring hydrogens were assigned isotropic thermal parameters $B = 5.0$ Å^2 and placed in positions calculated with the assumption of trigonal-planar geometry and a C–H bond distance of 0.95 Å. The hydrogen atoms of the solvent molecules could not be located; as the refinement progressed, disorder of the ethanol molecule became evident. The refinement was considered to have converged when the parameters of none of the atoms (except those of the disordered ethanol molecule) shifted more than 10% of their standard deviations (the shifts for the oxygen and carbon atoms in the ethanol molecule were less than 25% of the standard deviations). The maximum and minimum peaks in the final difference Fourier map were 1.03 and −0.61 e/Å^3. The final weighted and unweighted R factors are 7.8 and 5.0%, respectively. Positional and thermal parameters obtained in the final least-squares cycle are collected in Table II.

$[Et_3NH]_2[V(cat)_3] \cdot CH_3CN$. A sharpened Patterson function revealed the position of the vanadium ion. Subsequent cycles of refinement and difference Fourier synthesis afforded the positions of the remaining non-hydrogen atoms. Since the acetonitrile molecule was not well resolved, it was constrained to a linear structure with fixed CN and C–C distances. Refinement of all non-hydrogen atoms with anisotropic thermal parameters (except for the acetonitrile) converged to $R = 8.06$; the enantiomeric structure converged to $R = 8.88$%, indicating the original choice of chirality for this crystal specimen was correct. Inclusion of the hydrogen atoms at the positions calculated for them (with the acetonitrile atoms fixed) led to final convergence with $R = 5.84$%, $R_w = 7.38$%, and the goodness of fit 2.37 for 352 parameters and 3644 observations with $F_o^2 > 3\sigma(F^2)$. A final difference map showed no peak greater than 0.38 e$^-$/Å^3. Inspection of the final ΔF values showed no evidence of secondary extinction, and the residuals in ranges of $(\sin\theta)/\lambda$ and F showed no abnormal trends. Positional and thermal parameters obtained in the final least-squares cycle are collected in Table III.

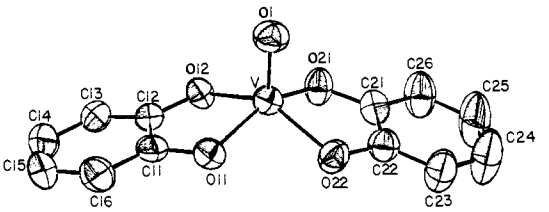

Figure 1. Molecular structure of the complex anion in $K_2[VO(cat)_2] \cdot EtOH \cdot H_2O$.

$K_3[V(cat)_3] \cdot 1.5H_2O$. The positional parameters of the isostructural Cr(III) complex were used as the starting point in the refinement. Final refinement with anisotropic thermal parameters for all non-hydrogen atoms gave $R = 3.5$% and $R_w = 4.6$% for 3422 data and 267 variables. The positions of the aromatic hydrogen atoms were calculated as above and assigned $B = 5.0$ Å^2; the hydrogens of the water molecule were not located. The maximum and minimum peaks in the final difference Fourier map were 0.50 and −0.32 e$^-$/Å^3. Positional and thermal parameters obtained in the final least-squares cycle are collected in Table IV.

Results and Interpretation

Description of the Structures. $K_2[VO(cat)_2] \cdot EtOH \cdot H_2O$. The bond distances and angles of the non-hydrogen atoms of $K_2[VO(cat)_2] \cdot EtOH \cdot H_2O$ (Figure 1, Table V) indicate that the coordination sphere of the anion closely approximates a square pyramid; the major deviation from C_{2v} symmetry is due to the larger bending of one catechol ring away from the apical oxygen than the other (the dihedral angles between the catechol ring and the corresponding chelate O–V–O plane are 15.6° and 9.9° for catechols 1 and 2, respectively). The vanadium ion is displaced toward the apical oxygen by 0.58 Å from the plane of the basal oxygens, and the two O–V–O planes make an angle of 133.0°, with a dihedral angle between the aromatic rings of 156.4°. The vanadyl V=O distance, 1.616 (4) Å, is in the 1.56–1.76-Å range reported for other vanadyl complexes.[27] The V–O(catechol)

(25) Freyberg, D. P.; Robbins, J. L.; Raymond, K. N.; Smart, J. C. *J. Am. Chem. Soc.* **1979**, *101*, 892–897.

(26) The following programs were used: MULTAN (direct methods), NUCLS (nonlinear least-squares refinement), FORDAP (Fourier calculations), ORFFE (bond distance and angle calculations), and ORTEP (thermal ellipsoid drawings). The analytical forms of the scattering factor tables for the neutral atoms were used throughout. (Cromer, D. T.; Waber, J. T. "International Tables for X-Ray Crystallography"; Kynoch Press: Birmingham, England, 1974; Vol. IV, Table 2.2B.) Corrections for the real and imaginary components of the anomalous dispersion for non-hydrogen atoms were made from Table 2.3.1 by D. T. Cromer in the above reference.

(27) (a) Selbin, J. *Chem. Rev.* **1965**, *65*, 153–175. (b) Selbin, J. *Coord. Chem. Rev.* **1966**, *1*, 293–314.

Table II. Positional and Thermal Parameters of $K_2VO(cat)_2 \cdot EtOH \cdot H_2O$

atom	x	y	z	β_{11}	β_{22}	β_{33}	β_{12}	β_{13}	β_{23}
V	−0.05745 (7)	0.12331 (7)	0.74524 (8)	0.00467 (5)	0.00475 (6)	0.00704 (9)	−0.00014 (5)	0.00222 (5)	0.00028 (6)
K1	−0.07891 (10)	0.10438 (10)	0.07520 (11)	0.00666 (9)	0.00539 (9)	0.00880 (13)	0.00058 (7)	0.00283 (9)	−0.00076 (8)
K2	0.10242 (11)	0.40386 (12)	0.06504 (14)	0.00803 (11)	0.0083 (12)	0.01197 (17)	0.00199 (9)	0.00560 (11)	0.00134 (11)
O11	0.03724 (26)	0.11108 (27)	0.92358 (31)	0.00523 (23)	0.00519 (26)	0.00723 (36)	−0.00022 (21)	0.00227 (24)	0.00037 (24)
O12	0.03273 (26)	0.24020 (28)	0.73787 (32)	0.00486 (24)	0.00568 (27)	0.00670 (36)	−0.00079 (19)	0.00134 (24)	0.00020 (24)
O21	−0.16374 (27)	0.20307 (31)	0.61170 (34)	0.00462 (24)	0.00754 (31)	0.00989 (42)	−0.00062 (22)	0.00184 (26)	0.00251 (29)
O22	−0.16379 (27)	0.09365 (31)	0.80709 (35)	0.00476 (24)	0.00874 (34)	0.00836 (38)	−0.00005 (22)	0.00281 (25)	0.00126 (29)
O1	−0.03343 (29)	0.01865 (30)	0.67475 (34)	0.00686 (29)	0.00613 (29)	0.01024 (43)	−0.00039 (22)	0.00389 (30)	−0.00097 (28)
O2	−0.10574 (42)	0.35450 (43)	0.91243 (43)	0.01197 (46)	0.01270 (52)	0.01287 (58)	−0.00019 (38)	0.00512 (42)	−0.00164 (42)
C11	0.12033 (40)	0.17047 (44)	0.94199 (48)	0.00509 (36)	0.00584 (39)	0.00760 (55)	0.00039 (31)	0.00262 (37)	−0.00127 (38)
C12	0.11608 (39)	0.24254 (42)	0.84328 (47)	0.00437 (32)	0.00571 (39)	0.00694 (51)	−0.00004 (28)	0.00227 (33)	−0.00051 (36)
C13	0.19501 (43)	0.31583 (52)	0.86223 (55)	0.00537 (38)	0.00897 (52)	0.00954 (63)	−0.00128 (37)	0.00367 (42)	−0.00054 (47)
C14	0.27985 (46)	0.30836 (58)	0.97413 (63)	0.00551 (42)	0.01052 (62)	0.01146 (73)	−0.00234 (41)	0.00313 (47)	−0.00193 (56)
C15	0.28667 (47)	0.23295 (65)	0.06883 (61)	0.00466 (41)	0.01359 (75)	0.01012 (73)	−0.00058 (44)	0.00084 (44)	−0.00263 (60)
C16	0.20704 (46)	0.16325 (53)	0.05401 (53)	0.00594 (42)	0.00902 (52)	0.00754 (53)	0.00109 (38)	0.00157 (40)	0.00135 (44)
C21	−0.25506 (43)	0.17401 (48)	0.61057 (56)	0.00511 (38)	0.00670 (45)	0.01035 (66)	−0.00047 (34)	0.00183 (41)	−0.00025 (45)
C22	−0.25541 (40)	0.11524 (46)	0.71626 (52)	0.00502 (36)	0.00646 (42)	0.00893 (58)	0.00012 (32)	0.00218 (37)	0.00037 (42)
C23	−0.34472 (48)	0.08523 (59)	0.72424 (67)	0.00522 (42)	0.01165 (66)	0.01336 (81)	−0.00048 (42)	0.00304 (48)	0.00196 (57)
C24	−0.43294 (53)	0.10859 (74)	0.62909 (87)	0.00521 (46)	0.01633 (94)	0.02117 (122)	−0.00140 (54)	0.00315 (62)	0.00527 (86)
C25	−0.43359 (53)	0.16952 (81)	0.52266 (86)	0.00474 (47)	0.01770 (100)	0.01966 (119)	−0.00026 (55)	−0.00023 (51)	0.00531 (90)
C26	−0.34397 (51)	0.20031 (58)	0.51271 (67)	0.00567 (45)	0.01064 (65)	0.01395 (84)	−0.00023 (42)	0.00078 (50)	0.00444 (59)
O3[a]	0.2413 (8)	0.0028 (9)	0.8178 (9)	15.7 (3)					
C31[a]	0.3449 (16)	−0.0062 (17)	0.8596 (18)	18.3 (6)					
C32[a]	0.3914 (14)	−0.0055 (18)	0.8010 (18)	19.0 (7)					

[a] Disordered ethanol molecule.

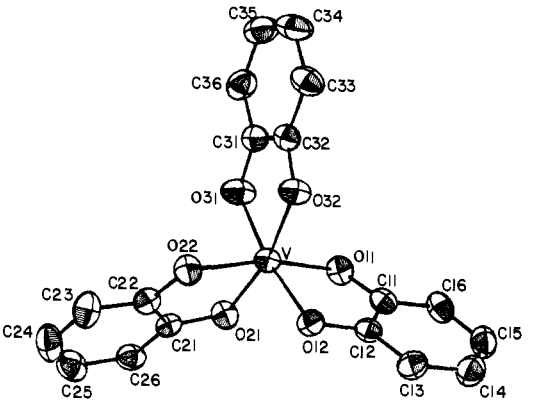

Figure 2. Molecular structure of the complex anion in $K_3[V(cat)_3] \cdot 1.5H_2O$.

distance (1.956 Å) is approximately 0.06 Å shorter for $K_2[VO(cat)_2] \cdot EtOH \cdot H_2O$ than that found for $K_3[V(cat)_3] \cdot 1.5H_2O$ (vide infra), as expected from the metal ionic radii for the two oxidation states [0.72 Å for V(IV) and 0.78 Å for V(III)[28]].

One potassium (K1) is coordinated by five catechol oxygen atoms, while the other is bound by two water molecules (O2), two vanadyl oxygen atoms (O1), and one catechol oxygen atom (O12).

The C–C bonds in the catechol rings of $K_2[VO(cat)_2] \cdot EtOH \cdot H_2O$ show little or no difference from those of the free ligand,[29] while the tris(catecholate) complexes of Fe(III), Cr(III),[30] V(III) (this work), and Si(IV)[31,32] and the tetrakis(catecholate) complexes of U(IV),[33] Th(IV),[33] Ce(IV),[20] and Hf(IV)[20] show differences from the ligand structure that are statistically significant. In general, the structures show little or no evidence for the quinone or semiquinone ligand structure. Thus the distortions

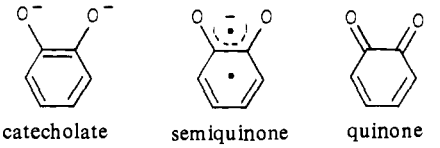

observed correspond to relatively small perturbations of the catecholate form of the ligand. This is in contrast to the semiquinone (or quinone) complexes.

$K_3[V(cat)_3] \cdot 1.5H_2O$. The $[V(cat)_3]^{3-}$ anion has essentially the same bond lengths and angles as the analogous Fe(III) and Cr(III) complexes (Figure 2, Table V).[30] However, comparison with the Fe(III), Cr(III), and V(IV) complexes shows slight differences in the five-membered chelate ring distances and angles, which can be ascribed to the greater ionic radius of the V(III) ion.

The dihedral angles between O–V–O planes and the aromatic rings are 10.4, 7.2, and 5.6° for rings 1 through 3, respectively. The O···O separation within the five-membered ring is 2.624 (2) Å, and the ligand bite (defined as the ratio of the O···O ring distance to the M–O distance) is 1.304. The trigonal twist angle is 45.6°.

$(Et_3NH)_2[V(cat)_3] \cdot CH_3CN$. $(Et_3NH)_2[V(cat)_3] \cdot CH_3CN$ has an approximately octahedral coordination geometry, with three bidentate catecholate ligands arrayed about the vanadium ion. The complex deviates considerably from rigorous octahedral geometry because of hydrogen bonding of the triethylammonium cations to two of the catechol oxygens (Figure 3, Table V). The

(28) Shannon, R. D. *Acta Crystallogr., Sect. A* **1976**, *32A*, 751–767.
(29) Wunderlich, V. H.; Mootz, P. *Acta Crystallogr., Sect. B* **1971**, *27B*, 1684–1686.
(30) Raymond, K. N.; Isied, S. S.; Brown, L. D.; Fronczek, F. R.; Nibert, J. H. *J. Am. Chem. Soc.* **1976**, *98*, 1767–1774.
(31) Flynn, J. J.; Boer, F. P. *J. Am. Chem. Soc.* **1969**, *91*, 5756–5761.
(32) Boer, F. P.; Flynn, J. J.; Turley, J. W. *J. Am. Chem. Soc.* **1968**, *90*, 6973–6977.
(33) Sofen, S. R.; Abu-Dari, K.; Freyberg, D. P.; Raymond, K. N. *J. Am. Chem. Soc.* **1978**, *100*, 7882–7887.

Table III. Positional and Thermal Parameters[a] of $(Et_3NH)_2V(cat)_3 \cdot CH_3CN$

atom	x	y	z	β_{11}	β_{22}	β_{33}	β_{12}	β_{13}	β_{23}
V	0.38759 (8)	0.66435 (8)	0.12869 (3)	0.01134 (7)	0.00936 (7)	0.00156 (1)	0.0010 (2)	−0.00231 (6)	0.00116 (6)
O11	0.3165 (3)	0.5865 (3)	0.1807 (1)	0.0117 (4)	0.0098 (3)	0.00179 (5)	0.0025 (6)	−0.0010 (2)	0.0020 (2)
O12	0.2389 (3)	0.7730 (3)	0.1383 (1)	0.0115 (3)	0.0110 (3)	0.00164 (5)	0.0035 (6)	−0.0009 (2)	0.0028 (2)
O21	0.5203 (3)	0.7360 (3)	0.1660 (1)	0.0135 (4)	0.0103 (4)	0.00137 (4)	−0.0018 (6)	−0.0026 (2)	0.0017 (2)
O22	0.4522 (3)	0.7871 (3)	0.0880 (1)	0.0133 (4)	0.0125 (4)	0.00130 (4)	−0.0040 (7)	−0.0016 (2)	0.0011 (2)
O31	0.4988 (3)	0.5203 (3)	0.1198 (1)	0.0131 (4)	0.0103 (3)	0.00170 (5)	0.0027 (6)	−0.0024 (2)	0.0003 (2)
O32	0.3001 (4)	0.5882 (4)	0.0791 (1)	0.0137 (4)	0.0123 (4)	0.00179 (5)	0.0012 (7)	−0.0029 (3)	0.0000 (3)
N4	0.1828 (5)	0.8956 (5)	0.0572 (1)	0.0184 (6)	0.0156 (6)	0.00149 (6)	0.009 (1)	−0.0032 (3)	−0.0004 (3)
N5	0.6398 (5)	0.4665 (5)	0.1954 (2)	0.0178 (6)	0.0189 (6)	0.00155 (6)	0.011 (1)	−0.0010 (4)	0.0019 (3)
N6	−0.0408 (0)	0.2579 (0)	0.1102 (0)	18.0000 (0)					
C11	0.2162 (5)	0.6428 (5)	0.1986 (2)	0.0130 (6)	0.0107 (6)	0.00149 (7)	−0.0028 (10)	−0.0015 (3)	0.0012 (4)
C12	0.1729 (5)	0.7460 (5)	0.1748 (2)	0.0115 (5)	0.0085 (5)	0.00164 (7)	0.0019 (9)	−0.0013 (3)	−0.0009 (3)
C13	0.0701 (6)	0.8112 (6)	0.1906 (2)	0.0163 (7)	0.0122 (7)	0.00201 (9)	−0.0003 (12)	−0.0030 (4)	−0.0003 (4)
C14	0.0076 (6)	0.7767 (6)	0.2298 (2)	0.0139 (7)	0.0167 (8)	0.00204 (9)	0.0015 (13)	−0.0016 (5)	−0.0016 (5)
C15	0.0523 (6)	0.6750 (7)	0.2526 (2)	0.0174 (8)	0.0177 (8)	0.00200 (9)	−0.0065 (15)	−0.0014 (4)	−0.0007 (5)
C16	0.1573 (6)	0.6077 (5)	0.2375 (2)	0.0160 (7)	0.0114 (6)	0.00174 (8)	−0.0006 (11)	−0.0015 (4)	0.0000 (4)
C21	0.5874 (5)	0.8304 (5)	0.1471 (2)	0.0114 (5)	0.0098 (5)	0.00151 (6)	−0.0024 (10)	−0.0004 (3)	0.0010 (3)
C22	0.5498 (5)	0.8549 (5)	0.1030 (2)	0.0114 (5)	0.0117 (6)	0.00131 (6)	0.0020 (10)	−0.0006 (3)	0.0002 (3)
C23	0.6110 (6)	0.9521 (5)	0.0803 (2)	0.0132 (6)	0.0152 (6)	0.00149 (7)	−0.0032 (12)	−0.0001 (4)	0.0029 (4)
C24	0.7074 (5)	1.0153 (6)	0.1012 (2)	0.0145 (7)	0.0127 (6)	0.00168 (8)	−0.0039 (12)	0.0014 (4)	0.0004 (4)
C25	0.7459 (6)	0.9882 (6)	0.1438 (2)	0.0135 (6)	0.0150 (7)	0.00200 (9)	−0.0048 (12)	0.0007 (4)	−0.0018 (4)
C26	0.6859 (5)	0.8935 (5)	0.1668 (2)	0.0148 (6)	0.0119 (6)	0.00149 (7)	−0.0028 (11)	−0.0018 (4)	−0.0000 (4)
C31	0.4674 (5)	0.4488 (5)	0.0846 (2)	0.0131 (6)	0.0102 (5)	0.00157 (7)	−0.0048 (10)	−0.0005 (4)	0.0017 (3)
C32	0.3560 (5)	0.4886 (5)	0.0618 (2)	0.0139 (7)	0.0098 (5)	0.00165 (7)	−0.0048 (10)	−0.0011 (4)	0.0011 (4)
C33	0.3143 (6)	0.4262 (6)	0.0243 (2)	0.0212 (9)	0.0120 (6)	0.00182 (9)	−0.0042 (13)	−0.0030 (5)	−0.0002 (4)
C34	0.3857 (8)	0.3232 (6)	0.0104 (2)	0.0298 (11)	0.0145 (7)	0.00177 (8)	−0.0109 (19)	−0.0001 (6)	−0.0001 (4)
C35	0.4957 (7)	0.2852 (6)	0.0321 (2)	0.0227 (9)	0.0149 (7)	0.00184 (9)	−0.0005 (15)	0.0016 (5)	−0.0003 (5)
C36	0.5357 (5)	0.3470 (5)	0.0694 (2)	0.0150 (7)	0.0119 (6)	0.00195 (8)	0.0019 (12)	0.0007 (4)	0.0002 (4)
C41	0.2210 (6)	0.8221 (7)	0.0190 (2)	0.0205 (8)	0.0196 (9)	0.00162 (8)	0.0092 (16)	−0.0034 (4)	0.0009 (5)
C42	0.2546 (9)	1.0243 (7)	0.0577 (3)	0.0317 (12)	0.0162 (9)	0.00272 (12)	−0.0054 (19)	−0.0055 (7)	0.0041 (5)
C43	0.0529 (7)	0.9177 (10)	0.0629 (3)	0.0221 (10)	0.0427 (15)	0.00280 (13)	0.0290 (21)	0.0019 (6)	0.0073 (7)
C44	0.1840 (8)	0.8746 (8)	−0.0256 (2)	0.0340 (13)	0.0263 (12)	0.00186 (10)	0.0183 (22)	−0.0042 (6)	0.0019 (6)
C45	0.2696 (8)	1.0715 (7)	0.1010 (3)	0.0266 (12)	0.0182 (9)	0.00286 (12)	−0.0052 (18)	−0.0001 (7)	−0.0048 (6)
C46	−0.0155 (9)	0.7860 (13)	0.0661 (3)	0.0204 (10)	0.0486 (21)	0.00411 (19)	−0.0246 (25)	−0.0045 (8)	0.0031 (11)
C51	0.5760 (6)	0.5126 (6)	0.2352 (2)	0.0188 (8)	0.0163 (7)	0.00167 (8)	0.0123 (13)	−0.0014 (4)	0.0019 (4)
C52	0.7684 (7)	0.5455 (10)	0.1919 (3)	0.0166 (9)	0.0379 (16)	0.00266 (12)	−0.0111 (21)	−0.0027 (6)	0.0071 (7)
C53	0.6722 (10)	0.3446 (8)	0.1927 (3)	0.0475 (16)	0.0182 (9)	0.00320 (14)	0.0329 (19)	−0.0042 (8)	−0.0048 (6)
C54	0.6427 (7)	0.4813 (8)	0.2793 (2)	0.0239 (10)	0.0254 (10)	0.00162 (8)	0.0147 (18)	−0.0014 (5)	0.0042 (5)
C55	0.8077 (7)	0.5659 (9)	0.1497 (3)	0.0163 (9)	0.0246 (12)	0.00436 (18)	−0.0019 (18)	0.0021 (7)	0.0024 (8)
C56	0.5432 (13)	0.2738 (8)	0.1935 (3)	0.0735 (29)	0.0137 (9)	0.00309 (15)	−0.0264 (27)	−0.0002 (12)	0.0022 (7)
C61	0.0397 (0)	0.3204 (0)	0.1252 (0)	17.5000 (0)					
C62	0.1400 (0)	0.3984 (0)	0.1440 (0)	16.0000 (0)					

[a] The form of the anisotropic thermal parameter is $\exp[-(\beta_{11}hh + \beta_{22}kk + \beta_{33}ll + \beta_{12}hk + \beta_{13}hl + \beta_{23}kl)]$.

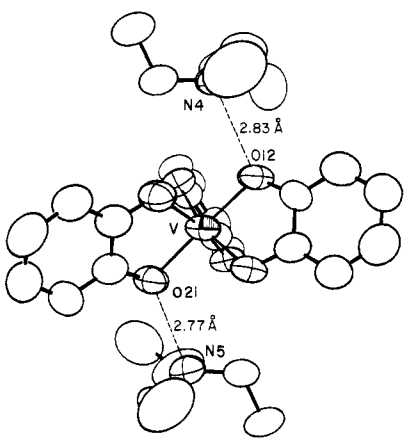

Figure 3. Molecular structure of the complex anion and its hydrogen bonding to the cation in $[Et_3NH]_2[V(cat)_3] \cdot CH_3CN$.

V–O bond lengths at 1.930 (3) Å are 0.07 Å shorter than those of the corresponding V(III) complex, consistent with the higher oxidation state of the former. The O–V–O bond angles are normal at 88.8°. The triethylammonium cations show a large degree of thermal motion.

Optical Spectra. $V^{IV}O(L)_2$ Complexes. The optical spectrum of $K_2[VO(cat)_2] \cdot EtOH \cdot H_2O$ (Figure 4A, Table VI) reveals d–d bands at 656 and 540 (sh) nm in water at pH ~ 12, with ϵ 69 and 38 M^{-1} cm^{-1}, respectively. By comparison, $[VO(Tironate)_2]^{2-}$ has the corresponding bands at 645 and 521 (sh) nm (Tiron is sodium 4,5-dihydroxy-1,3-benzenedisulfonate); $[VO(3,5\text{-di-}tert\text{-butylcatecholate})_2]^{2-}$ in MeOH (0.1 M in NaOH) has a band at 654 nm (ϵ 150). These results are typical for oxovanadium compounds, which have bands in the region 900–625, 690–520, and 470–330 nm[27] (ϵ 10–100, 5–50, and 5–100 M^{-1} cm^{-1}, respectively). The highest energy band in all cases is obscured by the tail of strong transitions in the ultraviolet, a common occurrence for vanadyl compounds (and catechols).

Our results for Tiron are in complete accord with those of Wüthrich for the 1:1 and 1:2 complexes.[34]

$V^{IV}(L)_3$ Complexes. The complex $[V(cat)_3]^{2-}$ in acetonitrile has two overlapping bands at 552 and 650 nm, with ϵ 9200 ± 200 and 8200 ± 200 M^{-1} cm^{-1}, respectively (Figure 4B); that of $[V(3,5\text{-di-}tert\text{-butylcatechol})_3]^{2-}$, prepared by chemical ($NaBH_4$) or electrochemical reduction of $[V(3,5\text{-di-}tert\text{-butylcatecholate})_3]^{-}$ in acetonitrile (vide infra), has the corresponding bands at 556 (ϵ 9200) and 660 nm (ϵ 8200) and is superimposable on that for $[V(cat)_3]^{2-}$ but for a very slight shift to lower energy for complexes of the alkylated ligand. In aqueous solution (pH 9) in the presence of excess ligand, the bands of the catechol complex shift slightly to 580 and ~675 nm. The corresponding bands of $[V(Tironate)_3]^{8-}$ in aqueous Tiron at pH 7 appear at 560 and 650 nm. It should be noted that the overlapping of the bands in all cases precludes precise band maximum measurements for the band at lower energy.

(34) Wüthrich, K. *Helv. Chim. Acta* **1965**, *48*, 1012–1017.

Table IV. Positional and Thermal Parameters[a] of $K_3V(cat)_3 \cdot 1.5H_2O$

atom	x	y	z	β_{11}	β_{22}	β_{33}	β_{12}	β_{13}	β_{23}
V	0.32499 (2)	0.01857 (3)	0.10648 (4)	0.00126 (1)	0.00253 (2)	0.00273 (2)	0.00008 (2)	0.00041 (3)	−0.00038 (4)
K1	0.06591 (3)	0.41867 (5)	0.11637 (6)	0.00169 (1)	0.00371 (3)	0.00458 (4)	−0.00036 (4)	0.00098 (4)	0.00059 (6)
K2	0.30889 (3)	0.13578 (5)	0.36445 (5)	0.00226 (2)	0.00321 (3)	0.00385 (4)	0.00017 (4)	0.00077 (4)	0.00025 (6)
K3	0.25805 (4)	0.40741 (6)	0.15843 (6)	0.00195 (2)	0.00567 (4)	0.00498 (5)	0.00103 (4)	−0.00093 (5)	−0.00347 (7)
O1	0.00000 (0)	0.5201 (2)	0.2500 (0)	0.00156 (7)	0.00285 (12)	0.0069 (2)	0.0000 (0)	0.0002 (2)	0.0000 (0)
O2	0.26296 (25)	0.2940 (2)	0.3541 (4)	0.01026 (18)	0.00584 (17)	0.0275 (6)	0.0086 (3)	−0.0158 (5)	−0.0105 (5)
O11	0.32320 (10)	0.1168 (1)	0.0070 (2)	0.00184 (5)	0.00284 (8)	0.0031 (1)	0.0004 (1)	−0.0005 (1)	−0.0000 (2)
O12	0.38504 (9)	0.0957 (1)	0.1930 (2)	0.00141 (4)	0.00268 (8)	0.0035 (1)	−0.0002 (1)	−0.0005 (1)	0.0008 (2)
O21	0.38956 (9)	−0.0372 (1)	0.0107 (1)	0.00178 (5)	0.000297 (9)	0.0033 (1)	0.0005 (1)	0.0015 (1)	0.0006 (2)
O22	0.34911 (10)	−0.0815 (1)	0.2027 (2)	0.00192 (5)	0.00285 (8)	0.0037 (1)	0.0004 (1)	0.0017 (1)	0.0006 (2)
O31	0.25436 (9)	−0.0425 (1)	0.0214 (2)	0.00142 (5)	0.00439 (10)	0.0053 (1)	−0.0000 (1)	0.0005 (1)	−0.0044 (2)
O32	0.25115 (9)	0.0486 (1)	0.1996 (2)	0.00133 (4)	0.00369 (9)	0.0036 (1)	0.0001 (1)	0.0002 (1)	−0.0018 (2)
C11	0.3502 (1)	0.1859 (2)	0.0524 (2)	0.00135 (6)	0.0029 (1)	0.0033 (2)	0.0007 (1)	0.0009 (2)	−0.0002 (2)
C12	0.3839 (1)	0.1744 (2)	0.1522 (2)	0.00113 (5)	0.0027 (1)	0.0034 (2)	0.0002 (1)	0.0006 (2)	0.0000 (2)
C13	0.4136 (1)	0.2428 (2)	0.2023 (3)	0.00173 (7)	0.0032 (1)	0.0048 (2)	−0.0003 (2)	−0.0003 (2)	−0.0002 (3)
C14	0.4108 (2)	0.3224 (2)	0.1540 (3)	0.00212 (8)	0.0030 (1)	0.0067 (2)	−0.0005 (2)	0.0011 (2)	−0.0011 (3)
C15	0.3787 (2)	0.3332 (2)	0.0566 (3)	0.00217 (8)	0.0026 (1)	0.0065 (2)	0.0006 (2)	0.0017 (2)	0.0013 (3)
C16	0.3479 (1)	0.2656 (2)	0.0057 (2)	0.00203 (7)	0.0030 (1)	0.0041 (2)	0.0012 (2)	0.0009 (2)	0.0012 (3)
C21	0.4102 (1)	−0.1113 (2)	0.0492 (2)	0.00119 (6)	0.0024 (1)	0.0037 (2)	−0.0005 (1)	0.0001 (2)	−0.0003 (2)
C22	0.3876 (1)	−0.1363 (2)	0.1518 (2)	0.00152 (6)	0.0026 (1)	0.0036 (2)	−0.0004 (2)	0.0003 (2)	−0.0007 (2)
C23	0.4060 (2)	−0.2137 (2)	0.1932 (3)	0.00285 (9)	0.0027 (1)	0.0050 (2)	−0.0002 (2)	0.0004 (2)	0.0006 (3)
C24	0.4469 (2)	−0.2660 (2)	0.1355 (3)	0.00296 (10)	0.0025 (1)	0.0070 (3)	0.0010 (2)	−0.0010 (3)	−0.0010 (3)
C25	0.4692 (2)	−0.2414 (2)	0.0371 (3)	0.00205 (8)	0.0034 (1)	0.0075 (3)	0.0012 (2)	−0.003 (2)	−0.0036 (3)
C26	0.4509 (1)	−0.1638 (2)	−0.0068 (2)	0.00145 (6)	0.0033 (1)	0.0049 (2)	0.0001 (2)	0.0007 (2)	−0.0018 (3)
C31	0.1957 (1)	−0.0273 (2)	0.0626 (2)	0.00144 (6)	0.0027 (1)	0.0040 (2)	−0.0000 (2)	0.0001 (2)	0.0003 (3)
C32	0.1942 (1)	0.0236 (2)	0.1557 (2)	0.00136 (6)	0.0027 (1)	0.0036 (2)	0.0003 (2)	0.0001 (2)	0.0009 (3)
C33	0.1354 (1)	0.0433 (2)	0.1996 (3)	0.00172 (7)	0.0043 (2)	0.0048 (2)	0.0011 (2)	0.0013 (2)	0.0001 (3)
C34	0.0789 (1)	0.0109 (2)	0.1527 (3)	0.00129 (6)	0.0055 (2)	0.0072 (3)	0.0005 (2)	0.0013 (2)	0.0023 (4)
C35	0.0804 (2)	−0.0413 (2)	0.0647 (3)	0.00154 (7)	0.0046 (2)	0.0074 (3)	−0.0009 (2)	−0.0006 (2)	0.0026 (4)
C36	0.1388 (2)	−0.0606 (2)	0.0195 (3)	0.00194 (7)	0.0034 (1)	0.0059 (2)	−0.0008 (2)	−0.0009 (2)	−0.0003 (3)

[a] The form of the anisotropic thermal parameter is $\exp[-(\beta_{11}hh + \beta_{22}kk + \beta_{33}ll + \beta_{12}hk + \beta_{13}hl + \beta_{23}kl)]$.

The high intensity of these bands and analogy with other metal catecholates (e.g., $[Fe(cat)_3^{3-}]$[30]) suggest that these transitions are most reasonably assigned as ligand-to-metal charge transfer in origin. Astakhov et al.[35] also reported V(IV) complexes with λ_{max} = 580 and 620 nm but made no attempt to assign the bands. [The latter band maximum is indicative of partial air oxidation (vide infra).]

$V^V(L)_3$ Complexes. The complex $[V(cat)_3]^-$, prepared by electrochemical oxidation of $[Et_3NH]_2[V(cat)_3] \cdot CH_3CN$ in acetonitrile, has bands at 625 nm (ϵ 13000) and 900 nm (ϵ 17000) (Figure 4C). Due to the similar visible absorption of $[V(cat)_3]^{2-}$ and $[V(cat)_3]^-$, the two complexes are exceedingly similar to the eye; they differ only in that $[V(cat)_3]^{2-}$ is subtly violet while $[V(cat)_3]^-$ is a clear blue. For [V(3,5-di-*tert*-butylcatecholate)$_3$]$^-$ in MeOH, the corresponding band appears at 645 nm (ϵ 13000) (Figure 4C).

$V^{IV}O(L)$ Complexes. The optical data in aqueous solution for the complexes VO(L) for the ligands catechol and Tiron again reveal great similarity. For catechol, bands appear at 750 and 550 nm (ϵ 33 and 28), and for Tiron, at 769 and 526 nm (ϵ 24 and 17) (Figure 4D, Table VI).[34]

Infrared Spectra. Vanadium(IV) Complexes. The salient difference between the infrared spectra of the V(IV) tris(catecholates) and the bis(catecholates) is the presence of the V=O stretch at 977 cm^{-1} for $[VO(3,5\text{-di-}tert\text{-butylcatecholate})_2]^{2-}$ (in $[VO(cat)_2]^{2-}$ there is a very broad band centered at 950 cm^{-1}; the V=O stretch may be a shoulder on this band at about 970 cm^{-1}); and the absence of this band in the corresponding tris complexes. This is in accord with the crystallographic results. Generally this stretch appears between 1035 and 935 cm^{-1}.[27] These low stretching frequencies imply substantial weakening of the V=O bond, consistent with strong σ and π electron donation by catechol to antibonding orbitals of the V=O group. A similar decrease in V=O stretching frequency has been reported for $Tl_2[VO(3,4\text{-dihydroxybenzaldehyde})_2]$, for which $\nu_{V=O}$ = 935 cm^{-1}.[12]

Although acetonitrile of crystallization is known to be present from the crystal structure and analytical data on $[Et_3NH]_2[V(cat)_3] \cdot CH_3CN$, no bands obviously attributable to the CN stretch were found in the 2200-cm^{-1} region. The otherwise unremarkable spectra are typical of catecholate complexes and are summarized in Table VII.

Electrochemistry. Aqueous Solutions—Catechol and Tiron. Cyclic voltammograms of a solution of a vanadyl salt in 0.1 M catechol (8 < pH < 11) at the hanging mercury drop electrode show a reversible reduction wave at E_f = −0.72 V vs. SCE, with separation between waves of 60 mV (independent of scan rate) and a peak current ratio near unity. Controlled potential coulometric measurements yield n = 1.0. The reduction is not reversible in solutions that lack excess catechol. The analogous experiment with Tiron yields a quasi-reversible wave at E_f = −0.43 V, with ΔE = 100 mV (6 < pH < 10); neither an increase in ligand concentration (to 0.2 M) nor an increase in pH sufficed to give a reversible wave.

These data reflect that for both ligands V(IV) tris complexes are formed, which are reduced in a simple fashion to the corresponding V(III) tris complexes. Because reduction of vanadyl compounds to the trivalent state entails loss of the vanadyl oxygen, such reductions are usually irreversible,[27,36] and no reversible reductions were found for any of the vanadyl complexes. The facile reductions observed here are, however, expected for tris chelates, in which no change in gross structure is involved. The anodic shift in reduction potential for the Tiron complex relative to that of catechol is consistent with the electron-withdrawing effect of the two sulfonate groups. Presumably the excess of ligand serves to maintain the integrity of the V(III) tris(catecholate), for which a smaller stability constant is expected than for V(IV); the V(III) tris complex of Tiron appears to be much less stable (as evidenced by the irreversible cyclic voltammogram) than that of catechol. This can be reasonably attributed to the very high charge of the former (a 9$^-$ ion) and is consistent with previous catechol systems we have studied.[20,30] Zelinka et al.[17] reported a wave for vanadium(IV) in the presence of catechol identical with that reported here but did not recognize that the tris complex was involved.

Acetonitrile Solutions—Catechol and 3,5-Di-*tert*-butylcatechol. Cyclic voltammetric examination of $(Et_3NH)_2[V(cat)_3] \cdot CH_3CN$

(35) Astakhov, A. I.; Klimenko, E. P.; Knyazeva, E. N.; Trachevski, V. V. *Russ. J. Inorg. Chem. (Engl. Transl.)* **1975**, *45*, 5-9.

(36) Lingane, J. J. *J. Am. Chem. Soc.* **1945**, *67*, 182-188.

Table V. Selected Distances (Å) and Angles (Deg) with Chemically Equivalent Averages[a]

bond	distance, Å: $K_3V(cat)_3 \cdot 1.5H_2O$	$(Et_3NH)_2V(cat)_3 \cdot CH_3CN$	$K_2VO(cat)_2 \cdot EtOH \cdot H_2O$
V-O11	1.984 (1)	1.921 (3)	1.963 (3)
V-O12	2.029 (1)	1.971 (2)	1.963 (4)
V-O21	2.012 (1)	1.944 (2)	1.962 (4)
V-O22	2.036 (1)	1.925 (3)	1.937 (4)
V-O31	2.026 (1)	1.961 (3)	
V-O32	1.993 (6)	1.931 (3)	
av V-O[b]	2.013 (9)	1.942 (8)	1.956 (6)
vanadyl V-O1			1.616 (4)
O11···O12	2.617 (2)	2.516 (3)	2.603 (5)
O21···O22	2.624 (2)	2.507 (3)	2.573 (5)
O31···O32	2.630 (2)	2.521 (4)	
av ring bite	2.624 (4)	2.515 (4)	2.588 (15)
O11-C11	1.347 (2)	1.327 (5)	1.352 (6)
O12-C12	1.346 (2)	1.326 (4)	1.336 (6)
O21-C21	1.335 (2)	1.361 (4)	1.359 (7)
O22-C22	1.346 (2)	1.334 (3)	1.361 (6)
O31-C31	1.351 (2)	1.348 (5)	
O32-C32	1.345 (2)	1.330 (5)	
av C-O	1.345 (2)	1.338 (6)	1.352 (6)
C11-C12	1.411 (2)	1.399 (5)	1.403 (7)
C21-C22	1.415 (2)	1.407 (5)	1.391 (8)
C31-C32	1.403 (3)	1.419 (5)	
av C1-C2	1.410 (4)	1.408 (6)	1.397 (6)
C12-C13	1.386 (3)	1.371 (6)	1.406 (7)
C11-C16	1.390 (3)	1.374 (6)	1.407 (7)
C22-C23	1.381 (3)	1.406 (5)	1.373 (8)
C21-C26	1.383 (3)	1.370 (5)	1.380 (8)
C32-C33	1.383 (3)	1.380 (6)	
C31-C36	1.386 (3)	1.388 (6)	
av C2-C3	1.385 (1)	1.382 (6)	1.392 (9)
C13-C14	1.398 (3)	1.395 (6)	1.392 (8)
C15-C16	1.391 (3)	1.393 (6)	1.393 (9)
C23-C24	1.396 (3)	1.371 (6)	1.353 (9)
C25-C26	1.393 (3)	1.384 (6)	1.390 (10)
C33-C34	1.391 (3)	1.404 (7)	
C35-C36	1.397 (3)	1.368 (6)	
av C3-C4	1.394 (1)	1.386 (6)	1.382 (10)
C14-C15	1.367 (3)	1.376 (7)	1.387 (9)
C24-C25	1.365 (3)	1.371 (6)	1.407 (11)
C34-C35	1.365 (3)	1.385 (7)	
av C4-C5	1.366 (2)	1.377 (4)	1.397 (10)
O11-V-O12	81.4 (1)	80.5 (1)	83.0 (1)
O21-V-O22	80.8 (1)	80.8 (1)	82.6 (2)
O31-V-O32	81.8 (1)	80.7 (1)	
av ring *cis* O-V-O	81.3 (3)	80.7 (1)	82.8 (2)
O11-V-O22	166.8 (1)	162.2 (1)	149.9 (2)[c]
O12-V-O31	170.5 (1)	164.0 (1)	141.1 (2)[c]
O21-V-O32	167.1 (1)	162.1 (1)	
av *trans* O-V-O	168.1 (1)	162.8 (6)	145.5 (44)

[a] Assuming D_3 point symmetry for the $V(cat)_3^{1-/2-}$ complexes and C_{2v} point symmetry for $VO(cat)_2^{2-}$. [b] Averages and their estimated standard deviations are calculated from the formula: $\bar{x} = (1/n)\Sigma_{i=1}{}^{n} x_i$; $\sigma(\bar{x}) = [(1/[n(n-1)])\Sigma_{i=1}{}^{n}(x_i - \bar{x})^2]^{1/2}$ or $\sigma(\bar{x}) = [\Sigma_{i=1}{}^{n} 1/\sigma_i^2]^{-1/2}$, whichever is greater. This corresponds to using either the observed variance or the least-square esd's as the estimators for $\sigma(\bar{x})$. [c] These angles are for O11-V-O21 and O12-V-O22 for the vanadyl structure.

in acetonitrile at a platinum disk electrode reveals an oxidation wave at −0.035 V, in addition to an irreversible reduction corresponding to that seen in Figure 5A. The oxidation is an essentially reversible one-electron process (ΔE = 65 mV, peak current ratio ≈1) for which n = 1.0. In the presence of Et_3N and excess catechol, the reduction also becomes reversible, with E_f = −0.86 V (Figure 5B).

It is somewhat surprising that the $[V(cat)_3]^{2-}$ to $[V(cat)_3]^{3-}$ reduction potential does not differ more between water and acetonitrile than the observed 0.14 V; usually the much poorer solvation offered anions by Lewis base solvents such as acetonitrile results in large cathodic shifts for reduction processes.[37] In the present case a clue is provided by the $(Et_3NH)_2[V(cat)_3]\cdot CH_3CN$ crystal structure, in which the triethylammonium groups are hydrogen bonded to the catechol oxygens. This interaction is apparently very strong, as reflected by the distortion observed in the structure, and, if it persists in solution, could explain the diminished shift in E_f between water and acetonitrile. The room temperature EPR spectrum of $(Et_3NH)_2[V(cat)_3]\cdot CH_3CN$ in acetonitrile provides evidence that the ion pairing does persist in solution (vide infra).

Table VI. Summary of Optical and EPR Data for Vanadium(IV) Catechol Complexes

complex	λ_{max}, nm (ϵ)	solvent	$\lvert A \rvert$, 10^{-4} cm^{-1}	$\langle g \rangle$
$VO(OH_2)_5^{2+}$	763, 625[a]	H_2O	107	1.97[b]
VO(cat)	750 (33), 550 (28)	H_2O	96	1.969
$VO(Tironate)^{2-}$	769 (24), 526 (17)[c]	H_2O	95	1.966
VO(DTBC)		MeOH	95	1.98
$VO(cat)_2^{2-}$	656 (69), 540 (38)	H_2O	82	1.977
$VO(Tironate)_2^{6+}$	645 (64), 521 (40)[c]	H_2O	80	1.972
$VO(DTBC)_2^{2-}$	654 (150)	EtOH (0.2 M NaOH)	77	1.970
$V(cat)_3^{2-}$	552 (9200), 650 sh (8200)	CH_3CN	75	1.958
$V(Tironate)_3^{8-}$	580, 675 sh	H_2O	*d*	*d*
	552, 650 sh	H_2O	*d*	*d*
$V(DTBC)_3^{2-}$	552 (9200), 650 (8200)	CH_3CN	75	1.966

[a] From ref 23. [b] This work. [c] From ref 33. [d] No EPR was observed for aqueous solutions of $V(cat)_3^{2-}$ or $V(Tironate)_3^{8-}$ at room temperature. DTBC is 3,5-di-*tert*-butylcatecholate.

Table VII. Infrared Spectral Data

$(Et_3NH)_2V(cat)_3\cdot CH_3CN$	$K_2VO(cat)_2\cdot EtOH\cdot H_2O$
3420b, 3050m, 3000m, 2975m, 2940w, 2660b, 2480b, 1960w, 1630w,b, 1569m, 1465s, 1450s, 1400m, 1365w, 1318w, 1300w, 1260s, 1223m, 1140w, 1095m, 1064w, 1030m, 1021m, 1013m, 935w, 895w,d, 870m, 840w, 801s, 732s, 620s,d, 552w, 532w, 500s, 442w, 413s, 364m, 310w	3510s, 3043w, 2575w, 1603m, 1570m, 1465s, 1310m, 1240s, 1145w, 1095m, 1014m, 920s, 863m, 853sh, 790s, 741sh, 732s, 628s, 510m, 423m, 380m

Thus, in consonance with the optical data, the electrochemical behavior of the vanadium(IV) complexes of 3,5-di-*tert*-butylcatechol in acetonitrile completely parallels that of the catechol complexes, which implies that 3,5-di-*tert*-butylcatechol also forms a tris complex, as has been proven for catechol itself. For the 3,5-di-*tert*-butylcatechol complex the potentials are shifted cathodically, as expected for electron-releasing alkyl groups.

No evidence was obtained for further reduction to divalent vanadium complexes.

Magnetic Behavior. The tris catechol complexes of V(IV) (L = catechol, Tiron, 3,5-di-*tert*-butylcatechol) exhibit magnetic moments (obtained by the NMR method) at 25 °C in accord with those expected for d^1, $S = {}^1/_2$ systems (1.73 μ_B). Similar magnetic behavior is observed for the mono and bis complexes of catechol and Tiron in aqueous solution and for those of 3,5-di-*tert*-bu-

(37) See, for example, Gutmann et al. [Gutmann, V.; Gritzner, G.; Danksagmüller, K. *Inorg. Chim. Acta* **1976**, *17*, 81-86] for the case of a trianion/tetraanion couple.

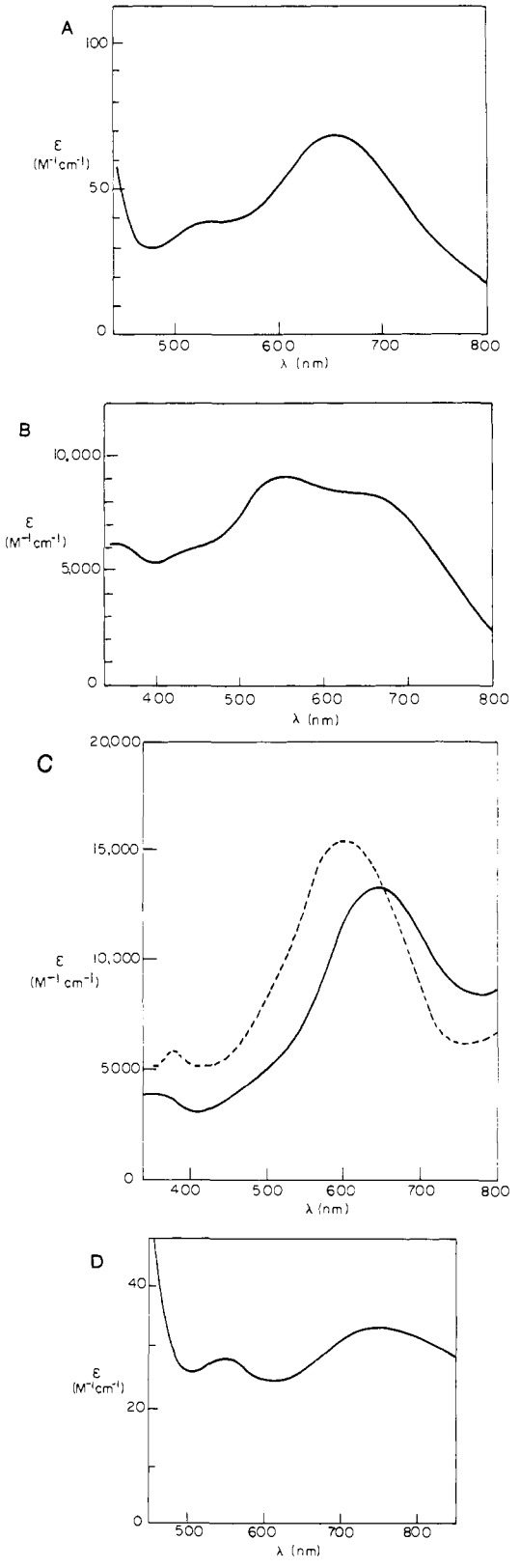

Figure 4. Optical spectra: (A) $K_2[VO(cat)_2]\cdot EtOH\cdot H_2O$ in aqueous 1 M KOH; (B) $[Et_3NH]_2[V(cat)_3]\cdot CH_3CN$ in CH_3CN; (C) of V(DTBC)$_3^-$ (solid line) and $[V(cat)_3]^-$ (dotted line) in CH_3CN, generated by electrochemical oxidation of the V(IV) complexes at a Pt mesh electrode; (D) $[VO(cat)]^0$ in H_2O.

tylcatechol in methanol or acetonitrile. The V(V) tris complexes are diamagnetic.

Electron Paramagnetic Resonance Spectra. Aqueous solutions of $VOSO_4$ exhibit an isotropic eight-line EPR spectrum at g = 1.97, with hyperfine coupling $A = 107 \times 10^{-4}$ cm^{-1} due to ^{51}V

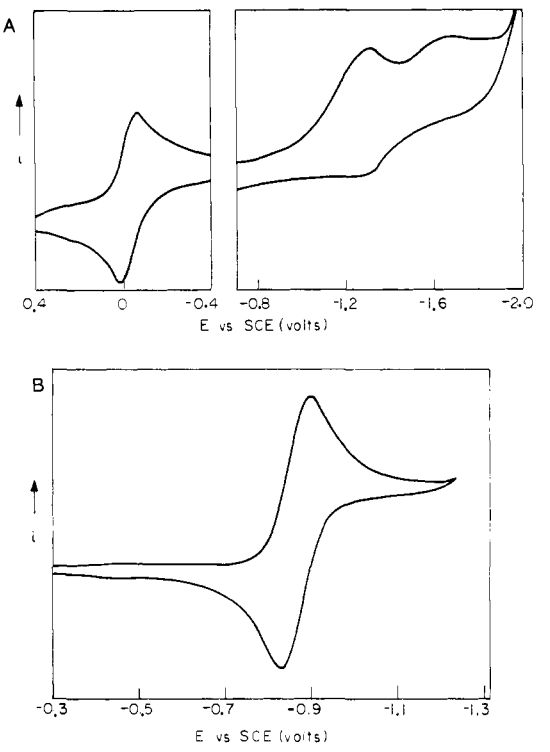

Figure 5. Cyclic voltammetric data: (A) $[V(cat)_3]^{2-}$ in CH_3CN solution; Pt electrode; (B) $[V(cat)_3]^{2-}$ in CH_3CN solution; hanging mercury drop electrode, in presence of excess Et_3N and catechol.

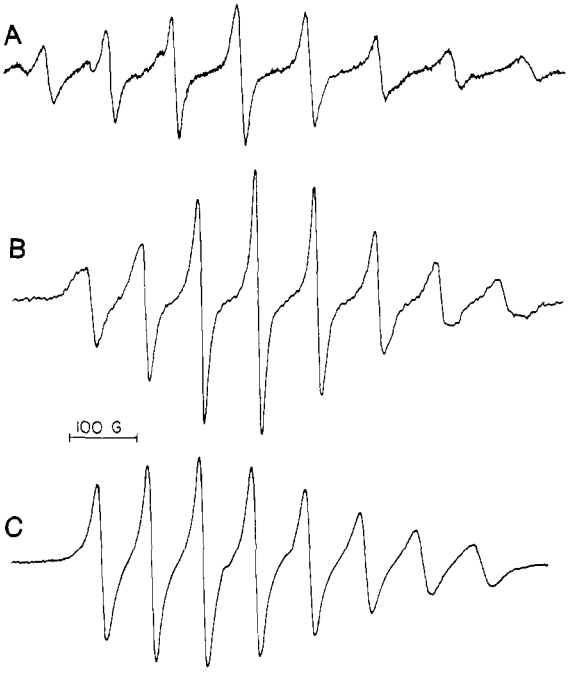

Figure 6. EPR spectra: microwave power 1 mW, modulation amplitude 5 G, DPPH as g standard: (A) VO(cat) (conditions as for optical spectrum); (B) $K_2[VO(cat)_2]\cdot EtOH\cdot H_2O$ in aqueous 1 M KOH; (C) $(Et_3NH)_2[V(cat)_3]\cdot CH_3CN$ in CH_3CN.

($I = {}^7/_2$, 100% abundant). Since the hyperfine coupling for V is significant with respect to the electronic Zeeman term, the EPR parameters reported in this paper (Table VI) have been corrected for second-order shifts in g and A values by nonlinear least-squares fitting to the second-order spin Hamiltonian:

$$\Delta E = \langle g\rangle \beta H + \langle A\rangle m_I + \frac{\langle A\rangle^2}{2\langle g\rangle \beta H}[I(I+1) + m_I^2]$$

In the presence of 2 equiv of catechol, the EPR spectrum of V(IV)

is pH dependent; the predominant species as a function of pH are as follows: at pH 3.2 the VO^{2+} aquo ion, at pH 4.2 a green complex with $A = 96 \times 10^{-4}$ cm^{-1} (Figure 6A), and above pH 6 a blue complex with $A = 82 \times 10^{-4}$ cm^{-1} (Figure 6B). At higher ligand-to-metal ratios a fourth, deep blue complex forms above pH 5, with concomitant disappearance of the EPR signal. Similarly, no EPR signal is observed for $(Et_3NH)_2[V(cat)_3]\cdot CH_3CN$ solutions in 0.1 M aqueous catechol (pH 9) under conditions in which the tris complex is known to remain intact from optical and magnetic data. Identical behavior is found for Tiron at somewhat lower pH values (Table VI). In marked contrast, an eight-line EPR signal with $A = 75 \times 10^{-4}$ cm^{-1} *is* observed for $(Et_3NH)_2[V(cat)_3]\cdot CH_3CN$ in *acetonitrile* (Figure 6C).

The pH dependence of aqueous solutions with 1:2 metal/ligand ratio is explained by successive coordination of the ligand to $[VO(OH_2)_4]^{2+}$, with the hyperfine splitting decreasing from the 107×10^{-4} cm^{-1} of the aquo ion to 96×10^{-4} cm^{-1} and then 82×10^{-4} cm^{-1} due to formation of [VO(L)] and $[VO(L)_2]$ (net charges of the complex depending upon the ligand L). This effect of ligand coordination upon hyperfine structure was first reported by Wüthrich for the mono and bis complexes of Tiron in an exceptionally lucid paper in 1965;[34] in contrast to the g values, the hyperfine values are sensitive to changes in the coordination sphere. We have extended Wüthrich's results on Tiron to the mono and bis complexes of catechol and 3,5-di-*tert*-butylcatechol and made use of these data in assigning the optical spectra of the $[VO(L)_n]$ series. Similar experiments with catechol and 3,5-di-*tert*-butylcatechol in acetonitrile and methanol (for which Et_3N was used as base) confirm the generality of this approach.

The peculiar solvent dependence of the EPR of the tris complex is particularly interesting. Coordination of a third catechol to the vanadyl bis(catecholate) raises the symmetry from square pyramidal to essentially octahedral and thereby generates an orbital triplet ground state. Ions with unquenched orbital angular momentum (T states) generally have very short electron spin relaxation times; the first-order spin–orbit coupling present in such ions efficiently couples the spin system to the lattice phonons by way of L, which is modulated by the lattice phonons.[38] In this fashion energy deposited in the spin system is rapidly dissipated in the lattice, which leads to a short spin relaxation time and hence very broad lines except at low temperature. Thus the disappearance of the room-temperature EPR signal (with retention of an experimentally verified $S = {}^1/_2$ magnetic moment) upon coordination of a third catechol can be understood. However, the EPR signal of what is unquestionably the tris complex *is* observed in acetonitrile (optical spectrum identical to that in H_2O, 1.7 μ_B magnetic moment). The solution to this puzzle is found in the crystal structure—hydrogen bonding of the triethylammonium hydrogens to the catechol oxygens leads to a distortion from octahedral symmetry. This distortion need only lift the degeneracy of the t_{2g} set by an energy $\sim kT$ to permit observation of the EPR spectrum at room temperature. Thus we consider the most reasonable explanation for observation of the room temperature spectrum of the tris complex in acetonitrile (but not in water or methanol) to reside in the inability of acetonitrile to compete with the triethylammonium cations for hydrogen bonding to the catechol oxygens.

Despite its paramagnetism (vide infra), $[V(cat)_3]^{3-}$ is EPR silent to 77 K, as expected for the non-Kramers' d^2, $S = 1$ configuration.[39]

Discussion

The tris(catecholato)vanadate(IV) ion in $(Et_3NH)_2[V(cat)_3]\cdot CH_3CN$ has a structure which to our knowledge is unprecedented for this oxidation state of vanadium—simple octahedral coordination, without the vanadyl (V=O) functionality. This previously unobserved phenomenon is attributed to the exceptional chelating ability of catechol, which is able in aqueous medium to displace the very stable vanadyl oxygen and achieve octahedral coordination at the metal center.

The results reported here on $[Et_3NH]_2[V(cat)_3]\cdot CH_3CN$ agree with the conclusion of Henry, Mitchell, and Prue[12] that the salt $Tl_2[V(cat)_3]$ is an octahedral tris complex, rather than a square-pyramidal vanadyl complex with catechol of crystallization. Although Henry et al. used a metal/ligand ratio of 1.8, essentially all the catechol was recovered as the tris complex (the excess vanadium presumably remained in solution). In this case the extreme insolubility of $Tl_2[V(cat)_3]$ drives tris complex formation to completion in the presence of thallium(I).

It is now possible to reconcile the controversy in the literature regarding the nature of vanadium(IV) catechol complexes—*both* octahedral tris and square-pyramidal bis complexes exist. The failure of the numerous potentiometric investigations to find evidence for this complex formation finds a ready explanation: apparently, none of the investigators recognized that, for the equilibrium involved:

$$VO(cat)_2^{2-} + catH_2 = V(cat)_3^{2-} + H_2O$$

no protons are consumed or liberated, and thus tris complex formation would not be apparent in a potentiometric experiment. It *would*, however, be apparent in a spectrophotometric experiment, which accounts for the discrepancy in the literature between the two sets of results. In basic solution the equilibrium

$$catH_2 + {}^-OH = catH^- + H_2O$$

becomes significant (pK_1 for catechol is 9.20, pK_2 is 11.93;[40] for Tiron pK_1 is 7.60, pK_2 is 12.48[41]) which leads to the overall reaction:

$$VO(cat)_2^{2-} + catH^- = V(cat)_3^{2-} + {}^-OH$$

Thus, in contrast to the usual case in catechol complex formation, at high pH mass action tends to force the equilibrium to *lower* catechol/vanadium ratios (to the left in the above equation), which explains the facile synthesis of vanadyl bis(catecholate) in strongly basic solution. Of course, in very strongly basic solution, where the catecholate *dianion* is produced, the above considerations obtain with still greater force.

In many of the studies in the literature no mention is made of whether the vanadium(IV) catecholate complexes (some of which are air sensitive) were protected from the atmosphere. The air oxidation of many of the complexes is slow, and in the case of $[V(cat)_3]^{2-}$ yields initially a blue product ($[V(cat)_3]^-$), which is very similar in appearance to the blue-violet starting material. For this reason the air sensitivity of this system was not always appreciated, and hence many of the results in the literature must be viewed with suspicion.

Shnaiderman[42] reported that vanadium(IV) in aqueous catechol solution formed a complex at pH 4–5 which did not migrate under the influence of an electric current and could be extracted from water with 1-butanol. From these observations and a Job's plot, he concluded that a neutral VO(cat) complex was formed, with water as the other two ligands. We have repeated these experiments and have identified the extracted complex to be indeed VO(cat) by means of optical and EPR spectra. Above pH 5 a second complex formed that migrated toward the anode, was not extractable by 1-butanol, and for which a Job's plot indicated 1:2 stoichiometry; accordingly, this complex was formulated as $[VO(cat)_2]^{2-}$.[42] Whether this complex was in fact the bis(catecholate) or the tris(catecholate) depends on the ligand to metal ratio used—observation of 1:2 stoichiometry is not conclusive because addition of the third catechol is relatively slow.[14]

The proton-dependent equilibrium constants K_1 and K_2

(38) Myers, R. J. "Molecular Magnetism and Magnetic Resonance Spectroscopy"; Prentice-Hall: Englewood Cliffs, NJ, 1973; p 194.
(39) Wertz, J. E.; Bolton, J. R. "Electron Spin Resonance: Elementary Theory and Applications"; McGraw-Hill: New York, 1972; pp 329–330.
(40) L'Heureux, G. A.; Martell, A. E. *J. Inorg. Nucl. Chem.* **1966**, *28*, 481–491.
(41) Martell, A. E.; Sillen, L. G. "Stability Constants"; Chemical Society: London, 1964; Special Publication No. 17, p 500.
(42) Shnaiderman, S. Ya. *Russ. J. Inorg. Chem.* (*Engl. Transl.*) **1963**, *8*, 239–244.

$$K_1 = \frac{[VO(cat)][H^+]^2}{[VO][catH_2]}$$

$$K_2 = \frac{[VO(cat)_2][H^+]^2}{[VO(cat)][catH_2]}$$

reported by Henry, Mitchell, and Prue[13] and Zelinka and Bartusek[11] are in good agreement. The corresponding proton-independent equilibria reported by these two groups differ only in their choice of protonation constants for the free ligand.

Nielson and Griffith[43] isolated complexes of catechol with Os(VI) which are of interest to compare with the present results. The neutral, diamagnetic, deep blue OsL_3 complexes, where L = catechol or 3,5-di-*tert*-butylcatechol, were found to be reversibly reduced in acetone at the dropping mercury electrode, at potentials (vs. Ag) of 0.04 and −0.72 V for L = catechol and 0.04 and −0.85 V for L = 3,5-di-*tert*-butylcatechol. Unfortunately, the authors do not specify the Ag^+ concentration of the reference and thus do not allow a quantitative comparison with the present results. However, it is apparent the behavior reported for the osmium complexes is qualitatively very similar to that observed for the tris complexes of vanadium(IV).

An interesting contrast to these results has been reported by Pierpont, Hendrickson, and collaborators[44] for the neutral tris complex of vanadium with tetrachloro-*o*-benzoquinone. This product, which was synthesized by reaction of tetrachloro-*o*-benzoquinone with $V(CO)_6$, exhibits an eight-line EPR spectrum at room temperature in ether with $\langle g \rangle = 2.0079$ and $\langle A \rangle = 4.1$ G and accordingly was formulated as a vanadium(III) tris(*o*-semiquinone) complex. While this is reasonable, an alternative formulation, which may warrant consideration, is that of a vanadium(V) bis(catecholate) *o*-semiquinone, in which either electron transfer or delocalization among the rings mediated by the metal (cf. the hyperfine coupling) may be significant. This suggestion is prompted by our observation of the tendency of "hard" catechol-like ligands to stabilize the highest accessible oxidation state of the metal [e.g., Ce(IV)[20]]. While it may be argued that tetrachloroquinone or 9,10-phenanthrenequinone are significantly different from catechol (or more accurately, *o*-benzoquinone), it will be noted that for the isolated complexes of these ligands, as well as catechol, the metal is in its highest accessible oxidation state [e.g., Mo(VI),[45,46] Cr(III),[30,45-48] Fe(III),[30,44] Ce(IV),[20] Ti(IV)[49]]. Furthermore, this complex may be considered to be derived from $[V(cat)_3]^-$ [which is certainly a V(V) complex, as demonstrated by its diamagnetism and LMCT band] by a one-electron oxidation, and introduction of four electron-withdrawing chloro groups (which would be expected to *increase* the tendency of the ligand to remove electron density from the metal). Thus, despite the gratifying pattern of trivalent metal complexes with three semiquinone ligands for Cr and Fe, for which the pentavalent oxidation state for vanadium is anomalous, in another sense the V(III) formulation disrupts the pattern of stabilization of the highest oxidation state of the metal.

Oxygen Binding. Recently Sawyer et al.[21] published a claim that methanolic solutions of vanadyl acetylacetonate and 3,5-di-*tert*-butylcatechol in 1:2 ratio reversibly bind oxygen, carbon monoxide, and nitric oxide. Our skepticism was provoked by a number of considerations. The various adducts reported by these workers had extremely similar optical spectra (superimposable in the cases of O_2 and CO) with a band maximum at 500 nm (the purple species in ref 21), an observation we considered most improbable. The infrared evidence for adduct formation cited by Sawyer et al. is equally questionable. Oxygen adduct formation was inferred from bands at 1135 and 890 cm^{-1}, which were assigned to vibrations of superoxo and peroxo groups, respectively. Such O–O vibrations, being highly variable in frequency and intensity, are notoriously difficult to assign in the absence of data from ^{18}O-substituted complexes. While we are puzzled as to the origin of the 1135-cm^{-1} band reported by Sawyer et al., the 890-cm^{-1} band is very close to the 892-cm^{-1} band of 3,5-di-*tert*-butylbenzoquinone, which is readily produced on exposure of the catechol to atmospheric oxygen, as in the experiment described by Sawyer and co-workers. On the other hand, no mention was made of the NO and CO stretching vibrations for these "adducts"—bands which are usually among the most prominent features of infrared spectra of NO and CO complexes.

Some of the observations of Sawyer et al. can be rationalized in terms of more prosaic phenomena than these authors apparently considered. For example, they reported that solutions of the NO and CO "adducts" are decolorized on exposure to oxygen to pale yellow solutions. Although not identified by these authors, this is obviously the quinone, which was produced by oxidation of catechol by O_2 or NO_2 (the latter being generated, of course, by interaction of NO and O_2, and is a common impurity in NO unless rigorously purified). It may also be noted that the species (with λ_{max} at 400 nm) that is generated by exposure of the blue solutions to oxygen and that Sawyer et al.[21] attributed to a "green species which results from further oxidation of the catechol" is also the quinone (there the green color is due to a mixture of the yellow quinone with the blue vanadium complex). On complete oxidation, only the yellow quinone remains (plus the very weakly absorbing vanadium), which accounts for the pale yellow solution reported by Sawyer et al. In a subsequent publication on molybdenum(VI) 3,5-di-*tert*-butylcatechol complexes, these workers apparently realized the identity of the species with λ_{max} at 400 nm as the corresponding quinone,[50] although this correction was never explicitly stated by them.

We have found that oxidation of $VO(acac)_2$ with benzoquinone, ammonium (hexanitrato)cerate(IV), hydrogen peroxide, or, more elegantly, by electrochemical means (Pt mesh electrode at +1 V vs. SCE) followed by catechol addition affords *under inert atmosphere* purple solutions with optical spectra identical with the "oxygen adduct" of Sawyer et al. [That is, O_2, NO, benzoquinone, Ce(IV), H_2O_2, and electrochemical oxidation all yield solutions with λ_{max} at 540 nm for catechol and 548 nm for 3,5-di-*tert*-butylcatechol; we are unable to account for the Sawyer report of the latter band at 500 nm]. Similarly, a solution of $VO(acac)_2$ and catechol can be oxidized with ferrocenium hexafluorophosphate under N_2 to yield an identical product. Our optical, electrochemical, and EPR results demonstrate conclusively that the di-*tert*-butyl derivative bears no significant difference from the parent catechol ligand. This result is expected, since the two ligands are, of course, extremely similar; the salient difference is that the electron-releasing effect of dialkyl substitution renders 3,5-di-*tert*-butylcatechol more susceptible to oxidation.[51] Other than a slight difference in position of band maxima (as expected), interaction with V(V) sources affords essentially the same purple species for both the parent ligand and its derivative. From the present work it is now clear that the optical spectrum of the supposedly tetrahedral species with λ_{max} 630 nm (before exposure to oxygen) is due to the $[V(3,5\text{-di-}tert\text{-butylcatecholate})_3]^{1-}$ ion. The alacrity with which this complex forms [by either oxidation of the V(IV) complex by adventitious oxygen or traces of the quinone in the easily oxidized ligand] and its high extinction coefficient require great care in the elimination of fallacious results

(43) Nielson, A. J.; Griffith, W. P. *J. Chem. Soc., Dalton Transl.* **1978**, 1501–1506.
(44) Buchanan, R. M.; Downs, H. H.; Shorthill, W. B.; Pierpont, C. G.; Kessel, S. L.; Hendrickson, D. N. *J. Am. Chem. Soc.* **1978**, *100*, 4318–4320.
(45) Pierpont, C. G.; Downs, H. H.; Rukavina, T. G. *J. Am. Chem. Soc.* **1974**, *96*, 5573–5574.
(46) Pierpont, C. G.; Buchanan, R. M. *J. Am. Chem. Soc.* **1975**, *97*, 6450–6455.
(47) Pierpont, C. G.; Downs, H. H. *J. Am. Chem. Soc.* **1976**, *98*, 4834–4838.
(48) Sofen, S. R.; Ware, D. C.; Cooper, S. R.; Raymond, K. N. *Inorg. Chem.* **1979**, *18*, 234–239.
(49) Cooper, S. R.; Raymond, K. N., manuscript in preparation.
(50) Reference 17 in Wilshire et al. (Wilshire, J. P.; Leon, L.; Bosserman, P.; Sawyer, D. T. *J. Am. Chem. Soc.* **1979**, *101*, 3379–3381).
(51) Ryba, O.; Pilar, J.; Petranek, J. *Collect. Czech. Chem. Commun.* **1968**, *33*, 26–34.
(52) **Note Added in Proof**: In a subsequent paper some of the original claims have been modified [Bosserman, P. J.; Sawyer, D. T. *Inorg. Chem.* **1982**, *21*, 1545–1551].

due to this complex. In the present study this was accomplished by thorough electrochemical or chemical reduction to obtain pure solutions of the [V(3,5-di-*tert*-butylcatecholate)$_3$]$^{2-}$ ion. It should be noted that the extinction coefficient reported by Sawyer et al. is less than half of the correct value for [V(3,5-di-*tert*-butylcatecholate)$_3$]$^{-}$; this indicates the extent of oxidation of the V(IV) starting material and implies that over half of the vanadium remained in the tetravalent state to give rise to the EPR spectrum (g = 1.98, A = 107.8 G) observed by Sawyer et al. It is likely that this EPR spectrum is due to unreacted VO(acac)$_2$, which has g = 1.969 and A = 105 G in the same solvent. Thus the data reported by Sawyer et al.[21] represent the *optical spectrum* of the V(V) complex with the *EPR spectrum* of a V(IV) complex. In the absence of base, [V(3,5-di-*tert*-butylcatecholate)$_3$]$^{2-}$ does not form in MeOH (similar results are obtained for catechol); presumably [V(3,5-di-*tert*-butylcatecholate)$_3$]$^{1-}$ *does* form because its higher metal ion charge leads to a higher stability constant, which permits it to displace the catechol protons without need for exogenous base.

More particularly, we have been able to identify the putative "oxygen adduct" as a vanadium(V) catechol complex. This complex is formed by reaction with NO or O_2, although not stoichiometrically in the former case; we have found that purple solutions generated by introduction of NO exhibit an EPR spectrum with *two* sets of hyperfine couplings (A = 107 and 97 $\times 10^{-4}$ cm^{-1}), which are characteristic of vanadyl acetylacetonate and mono(catecholate). Thus the "complicated EPR spectrum that is consistent with the patterns that have been observed for square-pyramidal geometry",[21] which Sawyer et al. attributed to superhyperfine splitting from the nitrogen of an axially symmetric NO ligand, is in fact due to a mixture of simple vanadyl complexes.

We have not in any of our experiments observed generation of the purple V(V) complex by exposure to pure CO as reported by Sawyer et al. and suggest that the improbable observation of superimposable optical spectra for both CO and O_2 adducts is more reasonably explained by exposure to oxygen in both cases.

Some of the more puzzling aspects of the report by Sawyer et al. remain unexplained—in particular the "reversibility" of "adduct formation", which we have not been able to reproduce. However, it is clear that the observations of Sawyer et al. are not due to reversible oxygen binding by vanadium catecholate complexes.

Acknowledgment. We wish to acknowledge the support of the NIH through Grant AI 11744. S.R.C. wishes to acknowledge the donors of the Petroleum Research Fund, administered by the American Chemical Society, for partial support of this research and to thank Professor E. J. Corey and K. Bloch of this department for use of their spectrophotometers. We also thank Dr. Frederick J. Hollander for his able experimental assistance and instruction in the structure analysis. Funds for the U.C.B. Chexray facility were provided by the NSF.

Registry No. [Et$_3$NH]$_2$[V(cat)$_3$]·CH$_3$CN, 82613-78-3; [Et$_3$NH][V(DTBC)$_3$], 82613-80-7; [Et$_3$NH]$_2$[VO(DTBC)$_2$], 82613-82-9; K$_2$[VO(cat)$_2$]·EtOH·H$_2$O, 82659-76-5; K$_3$[V(cat)$_3$]·1.5H$_2$O, 82613-84-1; VO(acac)$_2$, 3153-26-2; NH$_4$[VO$_3$], 7803-55-6; [V(DTBC)$_3$]$^{2-}$, 82613-85-2; [V(DTBC)$_3$]$^{-}$, 82613-86-3; [V(cat)$_3$]$^{-}$, 82613-87-4; VO(cat), 82598-73-0; [VO(Tironate)]$^{2-}$, 82613-88-5; VO(DTBC), 82598-74-1; [VO(Tironate)$_2$]$^{6-}$, 82621-18-9; [V(Tironate)$_3$]$^{8-}$, 82613-89-6.

Supplementary Material Available: Listing of observed and calculated structure factors (60 pages). Ordering information is given on any current masthead page.

Angle-Resolved Ultraviolet Photoelectron Spectroscopic Studies of CO Binding to Three Chemically Different Surfaces of ZnO. Confirmation of Step-Binding Sites on (000$\bar{1}$)

K. L. D'Amico, M. Trenary, N. D. Shinn, Edward I. Solomon,*[1] and F. R. McFeely*

Contribution from the Department of Chemistry, Massachusetts Institute of Technology, Cambridge, Massachusetts 02139. *Received December 7, 1981*

Abstract: Angle-resolved photoelectron spectroscopy (ARPES) has been performed on the ZnO(000$\bar{1}$)–CO system. These measurements are compared with previous ARPES results on (10$\bar{1}$0) and (0001) surfaces and strongly support earlier suggestions that the CO which is observed to chemisorb to this surface binds to (10$\bar{1}$0) step sites which contain coordinately unsaturated zinc ions but not to the (000$\bar{1}$) terrace sites which contain only coordinatively unsaturated oxide ions.

The adsorption of CO on ZnO is an important problem in relation to methanol synthesis.[2] The CO–ZnO bond is unusual because of the observation of a ~70-cm^{-1} *increase* in the CO stretching frequency upon chemisorption of CO on ZnO powders.[3] This is in contrast to the decrease in the stretching frequency relative to the gas-phase value of 2143 cm^{-1}, which is normally observed upon chemisorption to metals and in organometallic complexes. In an effort to gain a detailed microscopic understanding of the nature of the CO/ZnO interaction, we have recently reported a variety of ultraviolet photoelectron spectroscopic (UV PES) studies on four chemically different surfaces of ZnO:[4-6] (0001), which contains only coordinatively unsaturated zinc sites; (10$\bar{1}$0) and (11$\bar{2}$0), which contain both zinc and oxide ions with

(1) Present address: Department of Chemistry, Stanford University, Stanford, CA 94305.
(2) A. L. Waddams, "Chemicals from Petroleum", 3rd ed., Wiley, New York, 1973.
(3) (a) F. Boccuzzi, G. E. Garrone, A. Zecchina, A. Bossi, and M. Camia, *J. Catal.*, **51**, 160 (1978); (b) N. S. Hush and M. L. Williams, *J. Mol. Spectrosc.*, **50**, 349 (1974).
(4) R. R. Gay, M. H. Nodine, E. I. Solomon, V. E. Henrich, and H. J. Zeiger, *J. Am. Chem. Soc.*, **102**, 6752 (1980).
(5) M. J. Sayers, M. R. McClellan, R. R. Gay, E. I. Solomon, and F. R. McFeely, *Chem. Phys. Lett.*, **75**, 575 (1980).
(6) M. R. McClellan, M. Trenary, N. D. Shinn, M. J. Sayers, K. L. D'Amico, E. I. Solomon, and F. R. McFeely, *J. Chem. Phys.*, **74**, 4726 (1981).

0002-7863/82/1504-5102$01.25/0